FTIR spectroscopy of complexes formed between metarhodopsin II and C-terminal peptides from the G-protein α- and γ-subunits

Franz Bartl*, Eglof Ritter, Klaus Peter Hofmann[1]

Institut für Medizinische Physik und Biophysik, Universitätsklinikum Charité, Humboldt Universität zu Berlin, Ziegelstraße 5–9, D-10098 Berlin, Germany

Received 8 March 2000

Edited by Felix Wieland

Abstract Metarhodopsin II (MII) provides the active conformation of rhodopsin for interaction with the G-protein, Gt. Fourier transform infrared spectra from samples prepared by centrifugation reflect the pH dependent equilibrium between MII and inactive metarhodopsin I. C-terminal synthetic peptides (Gtα(340–350) and Gtγ(60–71)farnesyl) stabilize MII. We find that both peptides cause similar spectral changes not seen with control peptides (Gtα (K341R, L349A) and non-farnesylated Gtγ). The spectra reflect all the protonation dependent bands normally observed when MII is formed at acidic pH. Beside the protonation dependent bands, additional features, similar with both peptides, appear in the amide I and II regions.

Key words: Rhodopsin; Fourier transform infrared spectroscopy; Transducin; G-protein-coupled receptor; Signal transduction

1. Introduction

Rhodopsin absorbs photons to trigger the amplifying cascade of vision by coupling to the G-protein transducin (Gt). The light-sensitive ground state conformation of rhodopsin is stabilized by a salt bridge between the protonated Schiff base bond of the 11-*cis*-retinal to Lys^{296} and its counterion at Glu^{113} [1–3]. *Cis*/*trans* isomerization and relaxation through intermediates results in the protonation dependent 'metarhodopsin' states. Metarhodopsin I (MI), in which the Schiff base is still protonated, remains in a pH and temperature dependent equilibrium with the subsequent metarhodopsin II (MII) intermediate [3,4] which is the only form with a deprotonated Schiff base, reflected in its blue-shifted UV/Vis absorption [5]. The conversion to MII is coupled to proton transfer from the Schiff base, most likely to its counterion, Glu^{113} [2] and to proton uptake from solution, with the highly conserved residue Glu^{134} as the likely proton acceptor [6]. The kinetic difference between both reactions [7,8] and their decoupling in Glu^{134} mutants [6] have suggested that the two proton transfer events do not occur in one common proton relay but are rather thermodynamically coupled, yielding MII subforms MII_a and MII_b.

UV/Vis spectroscopy and photoregeneration experiments have shown that bound G-protein stabilizes MII (identified by its 380 nm absorption) at the expense of MI (forming 'extra MII'). Synthetic peptides from the Gtα and Gtγ C-terminal sequences can replace the Gt holoprotein in this regard [9], suggesting that the respective structures on the Gt holoprotein are interaction sites for rhodopsin. UV/Vis spectroscopy can provide information about the protonation state of the Schiff base but does not reflect directly the additional proton transfer reactions linked to MII formation. Fourier transform infrared (FTIR) difference spectroscopy allows to identify individual molecular changes that occur during photoproduct formation [10]. This study will show that such changes can be titrated as a function of pH in 'wet' samples prepared by centrifugation. The spectral features are compared to those induced by the binding of α- or γ-C-terminal peptides. Finally, the subtle differences between the spectra of the α- and γ-stabilized species will be considered.

2. Materials and methods

2.1. Isolation of bovine rod outer segments

Bovine reactive oxygen species (ROS) were prepared from fresh, dark-adapted retinas obtained from a local slaughterhouse by means of a discontinuous sucrose gradient method [11]. Retinas were dissected, and ROS were isolated under dim red illumination. All subsequent procedures were performed at 4°C.

2.2. Purification of rhodopsin

Rhodopsin membranes were prepared by removing the soluble and membrane-associated proteins from ROS membranes by repetitive washes with a low ionic strength buffer [12]. All steps were performed under dim red illumination. The membrane suspension was stored at −80°C until use.

2.3. Sample preparation

In a routinely applied preparation technique, a drop of the membrane suspension is dried onto an infrared (IR) transmissive material and rehydrated with a small amount of water [13,14]. This leads to very stable difference spectra, which are, however, in many cases insensitive to pH [15]. Generally, the capability of rhodopsin to form different intermediates depends crucially on the water content of the sample ([16] and own observations). Although the samples are rehydrated, irreversible changes in the hydration and thus protonation may occur. Even if the film is in contact with bulk water after the drying procedure (as for example in ATR spectroscopy [17,18]), the measured MI/MII equilibrium, by both the IR and the UV/Vis criteria, does not show the sensitivity to pH known from free membrane suspension (C. Meyer, E. Ritter and F. Bartl, unpublished observations).

We applied a centrifugation procedure according to [19], with mod-

*Corresponding author. Fax: (49)-30-2802 6377.
E-mail: franz.bartl@charite.de

[1] Also corresponding author. E-mail: klaus_peter.hofmann@charite.de.

Abbreviations: FTIR, Fourier transform infrared; MI, metarhodopsin I; MII, metarhodopsin II; G-protein, Gt, heterotrimeric guanine nucleotide binding protein; Gtα, Gtγ, α- and γ-subunits of Gt

PII: S0014-5793(00)01544-1

ifications. For a single experiment, ca. 70 μl of a 0.15 mM rhodopsin stock solution of washed membranes was used. For sample preparation, pH was adjusted by adding a few μl of diluted NaOH or HCl. Then the suspension was centrifuged for 25 min at 100 000×*g* to form a tightly packed pellet. The buffer solution was removed and the pellet was transferred to a 30 mm diameter BaF_2 window without any drying. The concentration of rhodopsin in the pellet was calculated to 2.2 mM by its visible absorbance spectra at 500 nm. The concentration was determined in the same sample and cuvette as used for IR spectroscopy. Then the window was assembled into a vacuum-sealed cell using a 5 μm PTFE-gasket and a second BaF_2 window, and placed into a temperature-controlled cell holder. For extra MII measurements, the rhodopsin pellet was resuspended in a 3 mM solution (100 μl) of the respective peptide. Then, after adjusting the pH as described, this suspension was centrifuged again for 25 min at 100 000×*g*. The final peptide concentration in the pellet was estimated

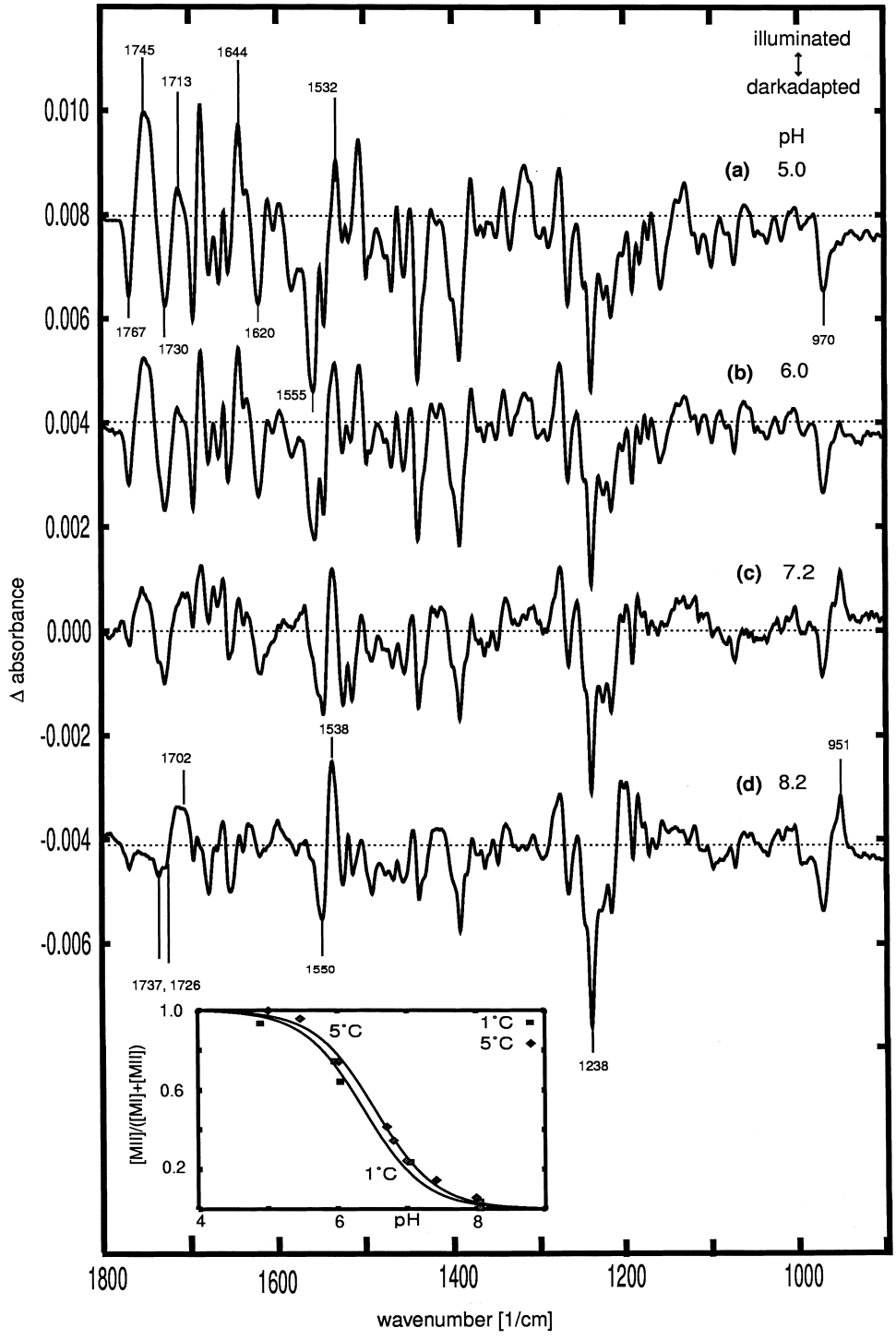

Fig. 1. FTIR analysis of the pH dependence of MII formation. FTIR difference spectra of [rhodopsin (illuminated)]−[rhodopsin (dark-adapted)] at 1°C, (a) pH 5.0, (b) pH 6.0, (c) pH 7.2, (d) pH 8.2. Spectra are arbitrarily shifted along the ordinate. Inset: [MII]/([MI]+[MII]) from a least square fit to difference spectra, plotted as a function of pH at 1°C and 5°C. Solid lines through the data are first order hyperbolic fits.

2.5 mM assuming that its amount was proportional to the water content.

2.4. Peptides

Peptide synthesis and purification were as described before [20]. The lyophilized peptides were dissolved in deionized water and the desired pH was adjusted with diluted NaOH.

Amino acid sequences for the peptides were as follows: Gtα(340–350), IKENLKDCGLF; high affinity analog (HAA) Gtα(340–350), VLEDLKSCGLF; Gtα(340–350) control, IRENLKDCGAF; Gtγ(60–71)farnesyl, DKNPFKELKGGC-farnesyl. Gtγ(60–71) control, DKNPFKELKGGC. The peptide is homogeneously dissolved in the suspension buffer.

2.5. FTIR measurements

All measurements were performed with a Bruker IFS 113v spectrometer using an LN_2-cooled HgMnTe-detector (EG&G Judson, J15D-series). Water content and equilibration were monitored by recording the intensity of the OH stretching vibration band at 3400 cm^{-1} during the experiment.

After an equilibration time of ca. 3 h, a set of 20 transmission spectra was recorded, each consisting of 64 scans. The sample was then photobleached for 20 s with a 150 W fiber-optic light source (LQ 1600, Spindler and Hoyer, Göttingen, Germany) operating at full power. 10 s after illumination, a second set of 20×64 scans was recorded under the same conditions. Spectra were setwise averaged and the difference spectrum was then generated by subtracting the spectrum of the dark-adapted sample from that of the illuminated sample. All difference spectra are the average of at least three different sets of spectra from separate samples. The proportion between MI and MII in the difference spectra was calculated by a least square fit, using MI and MII base spectra measured under the following conditions: MI: pH 8.2, $T=1$°C, yielding 99.4% MI; MII: pH 4.5, $T=10$°C, yielding 98.5% MII, according to [4].

3. Results

3.1. pH dependent FTIR difference spectra reflect the MI/MII equilibrium

We recorded two sets of FTIR difference spectra (spectrum after illumination minus spectrum of the dark-adapted sample) at pH values between 4.9 and 8.2, and temperatures 1°C and 5°C. A typical set of spectra recorded at 1°C is shown in Fig. 1. The spectrum at pH 5.0 and 1°C shows characteristic absorption bands in the spectral range between 1780 cm^{-1} and 1700 cm^{-1} where the C=O stretching vibrations of protonated carbonyl groups appear. The bands at 1767 cm^{-1} (negative, (−)) and 1745 cm^{-1} (+), and at 1730 cm^{-1} (−) are caused by changes in hydrogen bonds of Asp^{83} and Glu^{122} and the positive band at 1713 cm^{-1} (+) is due the protonation of the Schiff base counterion Glu^{113}. The strong positive absorptions at 1644 cm^{-1} and at 1532 cm^{-1} and negative bands at 1620 cm^{-1} and 1555 cm^{-1} can also be assigned to MII and show that the intermediate MII is formed quantitatively under these conditions [10]. With increasing pH, one observes the rise of the positive bands at 951 cm^{-1}, 1538 cm^{-1}, 1702 cm^{-1}, of the negative doublet at 1737 cm^{-1} and 1726 cm^{-1}, and of a negative band at 1550 cm^{-1}, all indicating a growing amount of MI [21]. Control UV/Vis spectra were recorded from identical samples, or aliquots, with the same result (data not shown).

The Inset in Fig. 1 shows the relative amount of MII as a function of pH, from a least squares fit to the IR spectra recorded at 1°C and 5°C. Hyperbolic fits to the data (solid lines) yield titration curves with apparent pK_a values 6.38 and 6.54 for 1°C and 5°C, respectively, in agreement with the MI/MII equilibrium [4].

3.2. Both, Gtα and Gtγ peptides affect the protonation dependent MI/MII equilibrium

Having established the pH dependence of MII in FTIR, we went on to examine the influence of Gtα- and of Gtγ-derived peptides on the pH dependent MI/MII equilibrium. This extends existing FTIR information on the effect measured with different analogs of the Gtα-derived C-terminal peptide using ATR spectroscopy [18] or transmission spectra at low temperatures [19].

Fig. 2a shows experiments with Gtα(340–350) peptides. In the absence, a virtually pure MI difference spectrum (see above) is seen, as expected under the conditions (pH 8.2, 1°C; Fig. 2a (dotted line)). In the presence of a saturating amount of Gtα(340–350) peptide (Fig. 2a, solid line), a clear MII spectrum is seen, including all features observed at acidic pH. This demonstrates that the Gtα(340–350) peptide is effective in stabilizing MII. The same difference spectra were measured with the HAA of the Gtα-derived peptide (data not shown). The difference spectra in the absence and presence of a Gtα(340–350) control peptide (Fig. 2b, dotted and solid lines, respectively; pH 8.2 and 1°C) are identical within the accuracy of the measurement, indicating the expected lack of an effect towards MII formation [9]. It also proves that no unspecific interaction of the peptides with the labile MI/MII equilibrium occurs.

The spectrum recorded with the γ-peptide (solid line in Fig. 2c) displays all characteristic MII features as described in Fig. 1a, demonstrating that the γ-derived peptide is also able to stabilize MII. For comparison, the difference spectrum of the peptide-free sample is shown (dotted line in Fig. 2c, same as in Fig. 2a). A control peptide lacking the farnesyl moiety has no effect on extra MII formation in UV/Vis spectroscopy [9]. Fig. 2d shows the analogous behavior in FTIR.

3.3. Comparison of MII and extra MII spectra

Fig. 3 compares spontaneously formed MII at pH 5.5 with extra MII at pH 8.2 and 1°C, induced by native Gtα- and Gtγ-far peptides. The subtracted spectra of the complexes with Gtα and Gtγ peptide show a conserved pattern in the amide I region between 1700 cm^{-1} and 1620 cm^{-1}, which indicates that the complex formation with Gtα and Gtγ peptide induces similar structural changes. The negative bands at 1687 cm^{-1} and 1642 cm^{-1} are accompanied with a positive band at 1657 cm^{-1}.

The bands from 1480 cm^{-1} to 1580 cm^{-1} cover the structurally sensitive amide II region (a coupled mode including C–N stretching and N–H bending vibrations). For the complexes with peptides, the amide II region shows characteristic bands at 1572 cm^{-1} (−), 1529 cm^{-1} (−) and 1551 cm^{-1} (+), in agreement with [19]. The MII/Gtγ-far complex does not show the negative bands at 1572 cm^{-1} and at 1529 cm^{-1} to the extent seen with the α-peptide, but shares the positive band at 1551 cm^{-1}.

4. Discussion

4.1. Gtα and Gtγ C-terminal peptides evoke the FTIR bands of MII

The data show that pH titration of FTIR samples yields an ensemble of spectral features that follows the pH and temperature dependence known from UV/Vis spectrophotometry [4] and proton uptake [7]. The spectral fingerprint of protonated

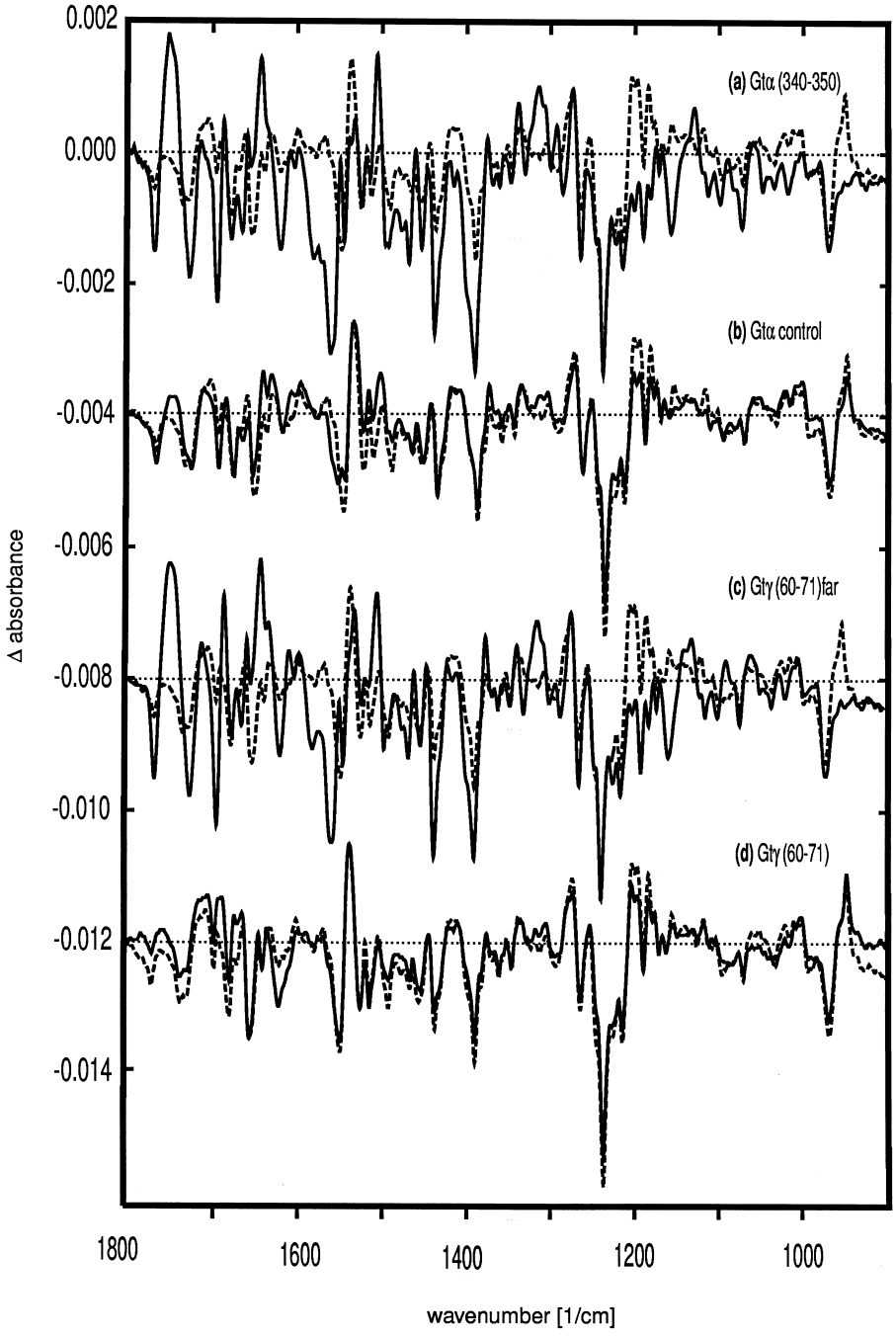

Fig. 2. Extra MII formation by interaction with the Gtα C-terminal peptide. a: solid line: FTIR difference spectra of [rhodopsin (illuminated)]−[rhodopsin (dark-adapted)] at 1°C and pH 8.2 in the presence of Gtα(340–350) native peptide (IKENLKDCGLF); dotted line: difference spectra in the absence of peptide, under the same conditions. b: solid line: FTIR difference spectra of [rhodopsin (illuminated)]−[rhodopsin (dark-adapted)] at 1°C and pH 8.2 in the presence of Gtα(340–350)-derived control peptide (IRENLKDCGAF); dotted line: difference spectra in the absence of peptide, under the same conditions. c: dotted line: FTIR difference spectra of [rhodopsin (illuminated)]−[rhodopsin (dark-adapted)] at 1°C and pH 8.2, in the presence of Gtγ(60–71)farnesyl-derived peptide; solid line: FTIR difference spectra of [rhodopsin (illuminated)]−[rhodopsin (dark-adapted)] at 1°C and pH 8.2 in the presence of (DKNPFKELKGGC-farnesyl). d: dotted line: FTIR difference spectra of [rhodopsin (illuminated)]−[rhodopsin (dark-adapted)] at 1°C and pH 8.2. solid line: FTIR difference spectra of [rhodopsin (illuminated)]−[rhodopsin (dark-adapted)] at 1°C and pH 8.2 in the presence of Gtγ-derived control peptide (same peptide as in c, without farnesyl group).

MII thereby obtained includes not only the proton translocation at the retinal Schiff base but also the related structural changes reflected in the reorientation of hydrogen bonds. This information provided the basis for comparing the protonated and peptide-stabilized forms of MII.

The data have shown that the Gtα and Gtγ C-terminal peptides fail to stabilize any species other than the protonated MII, as it is spontaneously formed at low pH. Protonation dependent spectral features include the band at 1713 cm^{-1}, indicating the protonation of the Schiff base counterion Glu^{113}, and the features reflecting changes in hydrogen bonding of residues Asp^{83} and Glu^{122}. Properties of Schiff base

protonated (i.e. MI-like) species are not detectable. Thus the data do not support a role of the MII subform MII_a [7] or of a MI-like species (MI_b [22]) in the two site interaction [9] with Gt. This does not exclude that binding sites other than the α- and γ-C-termini [23] may interact with earlier intermediates.

4.2. Peptide interaction sites at MII

The specific stabilization of protonated MII by both peptides tested implies that these short stretches from the Gtα and Gtγ sequences have the capacity to recognize the protonated MII species and to distinguish it from the other intermediates. A small percentage of the free peptide may have a conformation that fits better to protonated MII than to MI and the other intermediates [24]. Alternatively, the related receptor binding sites form a non-linear epitope only in MII. Light-induced microstructural changes were indeed detected by EPR and specified for the MII state [25], and the exposure of an epitope for an antibody specific for the light-activated state has been described [26].

Recent analyses draw attention to the fourth cytoplasmic loop of rhodopsin. With the same Gtα and Gtγ peptides as in the present investigation, a stabilizing effect was found as long as an intact fourth loop structure was present, independent of whether the primary sequence was from rhodopsin or the β_2 receptor [27]. An FTIR analysis of these mutants may offer the chance to elucidate the mechanism of interaction. Binding

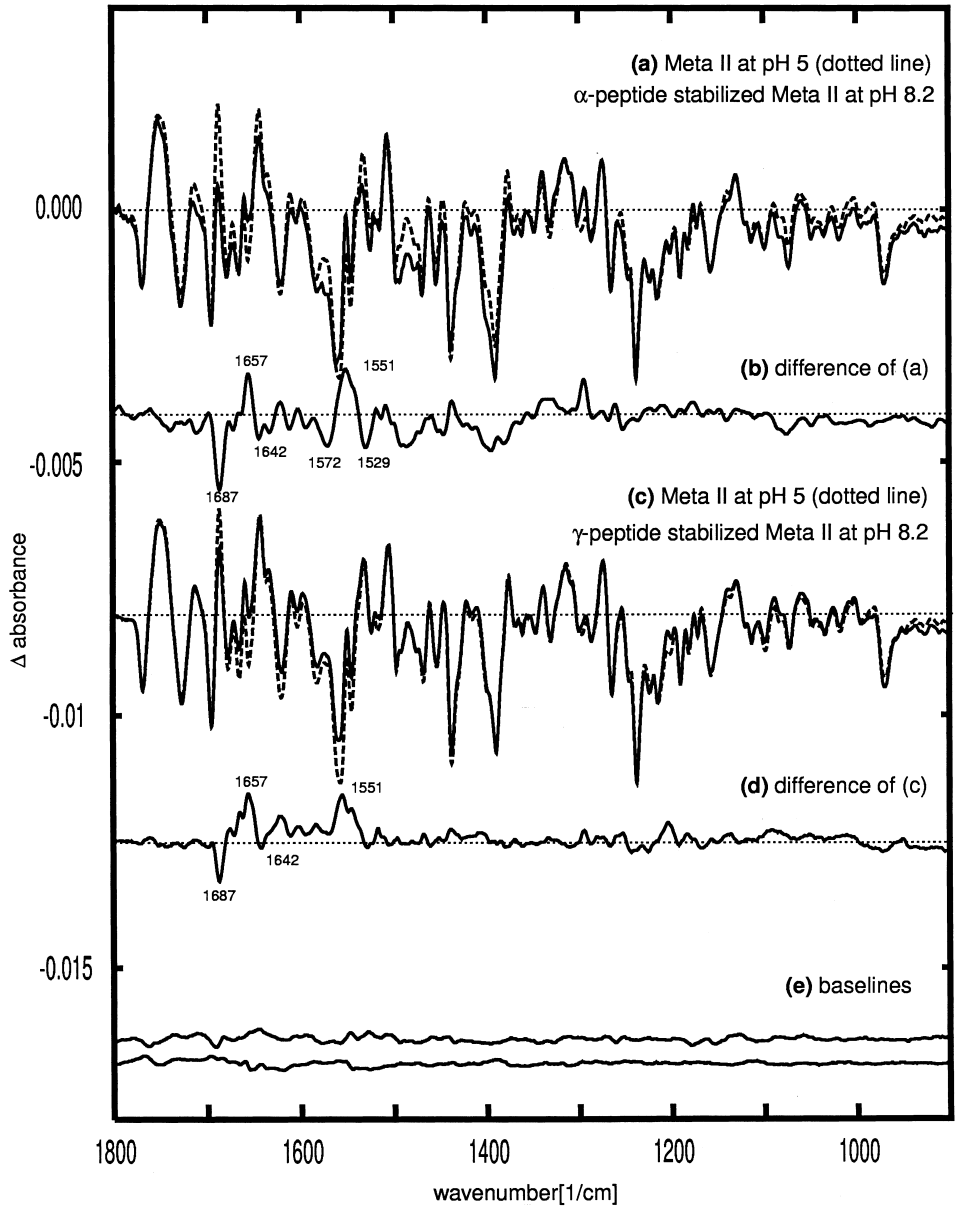

Fig. 3. Comparison of spontaneously formed MII (pH 5.0) with extra MII formed by peptide interaction (pH 8.2). Dotted lines in a and c: difference spectrum [rhodopsin (illuminated)]−[rhodopsin (dark-adapted)] at 1°C, pH 5.0, identical to Fig. 1a, for comparison. a: solid line: difference spectrum with Gtα(340–350) native peptide (same as in Fig. 2a); b: subtraction of the spectra in a: [extra MII−spontaneously formed MII]. c: solid line: difference spectrum with Gtγ(60–71)farnesyl-derived peptide (same as in Fig. 2a); d: subtraction of the spectra in c: [extra MII−spontaneously formed MII]. e: Baselines obtained by subtraction of two spectra recorded under the following conditions: top: subtraction of two rhodopsin/MII difference spectra, bottom: subtraction of two rhodopsin/MI spectra with and without control peptide.

of Gt to R* depends also on an intact second and third cytoplasmic loop [28]. A most critical region is close to the likely proton acceptor, Glu^{134}. FTIR features that appear in polarized IR difference spectra have now been tentatively assigned to Glu^{134} [29], and peptide stabilization experiments with this technique may be envisaged.

4.3. Differences between the peptide-induced spectral changes

The subtracted spectra in Fig. 3 show that the interaction between the peptides and photoactivated rhodopsin induces some positive and negative bands that do not appear in the pH dependent spectra. With the α-peptide, specific motifs appear in the amide I and amide II regions. These features, which are also seen with the γ-peptide, although less pronounced, indicate changes of secondary structure. The negative bands at 1687 cm^{-1} and at 1642 cm^{-1} could indicate turn and bend conformations of the peptide before binding to the receptor [30]. An induced formation of an α-helical binding motif in the Gtα peptide was deduced from nuclear magnetic resonance transfer NOESY spectroscopy [31]. The peptide-induced FTIR band at 1657 cm^{-1} (see Fig. 3) was accordingly assigned to an induced formation of α-helix [19]. Our results would then suggest that a similar event occurs with the γ-peptide. This structure has a role in both membrane anchoring and interaction with the receptor (see [32] and citations therein). Conceivably, the transition from the membrane to the receptor bound state could induce a more helical conformation of the C-terminal Gtγ structure, but it cannot be excluded that such a structural change occurs in the related receptor site. To discriminate between the two possibilities, labeled peptides will have to be applied.

Acknowledgements: We thank Dr. Peter Henklein for providing the peptides and Christoph K. Meyer for critical reading of the manuscript. We are grateful to Thorsten Evers for his help with the optical setup and Christine Koch for technical assistance. This study was supported by Grants to K.P.H. from the Deutsche Forschungsgemeinschaft (SFB 366) and from the Fonds der Chemischen Industrie.

References

[1] Cohen, G.B., Oprian, D.D. and Robinson, P.R. (1992) Biochemistry 31, 12592–12601.
[2] Sakmar, T.P. (1998) Prog. Nucleic Acid Res. Mol. Biol. 59, 1–34.
[3] Hofmann, K.P. (1999) in: Proceedings of the 224th Symposium of the Novartis Foundation, pp. 158–180, Wiley, Chichester.
[4] Parkes, J.H. and Liebman, P.A. (1984) Biochemistry 23, 5054–5061.
[5] Doukas, A.G., Aton, B., Callender, R.H. and Ebrey, T.G. (1978) Biochemistry 17, 2430–2435.
[6] Arnis, S., Fahmy, K., Hofmann, K.P. and Sakmar, T.P. (1994) J. Biol. Chem. 269, 23879–23881.
[7] Arnis, S. and Hofmann, K.P. (1993) Proc. Natl. Acad. Sci. USA 90, 7849–7853.
[8] Szundi, I., Mah, T.L., Lewis, J.W., Jager, S., Ernst, O.P., Hofmann, K.P. and Kliger, D.S. (1998) Biochemistry 37, 14237–14244.
[9] Kisselev, O.G., Meyer, C.K., Heck, M., Ernst, O.P. and Hofmann, K.P. (1999) Proc. Natl. Acad. Sci. USA 96, 4898–4903.
[10] Siebert, F. (1995) Isr. J. Chem. 35, 309–323.
[11] Papermaster, D.S. (1982) Methods Enzymol. 81, 48–52.
[12] Kühn, H. (1982) Methods Enzymol. 81, 556–564.
[13] Clark, N.A., Rothschild, K.J., Luippold, D.A. and Simon, B.A. (1980) Biophys. J. 31, 65–96.
[14] Siebert, F., Mäntele, W. and Gerwert, K. (1983) Eur. J. Biochem. 136, 119–127.
[15] Klinger, A.L. and Braiman, M.S. (1992) Biophys. J. 63, 1244–1255.
[16] Ganter, U.M., Schmid, E.D. and Siebert, F. (1988) J. Photochem. Photobiol. B Biol. 2, 417–426.
[17] Marrero, H. and Rothschild, K.J. (1987) Biophys. J. 52, 629–635.
[18] Fahmy, K. (1998) Biophys. J. 75, 1306–1318.
[19] Nishimura, S., Kandori, H. and Maeda, A. (1998) Biochemistry 37, 15816–15824.
[20] Kisselev, O.G., Ermolaeva, M.V. and Gautam, N. (1994) J. Biol. Chem. 269, 21399–21402.
[21] Ganter, U.M., Schmid, E.D., Perez Sala, D., Rando, R.R. and Siebert, F. (1989) Biochemistry 28, 5954–5962.
[22] Tachibanaki, S., Imai, H., Terakita, A. and Shichida, Y. (1998) FEBS Lett. 425, 126–130.
[23] Bae, H., Carbrera Vera, T.M., Depree, K.M., Graber, S.G. and Hamm, H.E. (1999) J. Biol. Chem. 274, 14963–14971.
[24] Dyson, H.J. and Wright, P.E. (1995) FASEB J. 9, 37–42.
[25] Farrens, D.L., Altenbach, C., Yang, K., Hubbell, W.L. and Khorana, H.G. (1996) Science 274, 770–786.
[26] Abdulaev, N.G. and Ridge, K.D. (1989) Proc. Natl. Acad. Sci. USA 95, 12854–12859.
[27] Ernst, O.E., Meyer, C.K., Marin, E.P., Henklein, P., Fu, W.Y., Sakmar, T.P. and Hofmann, K.P. (2000) J. Biol. Chem. 275, 1937–1943.
[28] Franke, R.R., König, B., Sakmar, T.P., Khorana, H.G. and Hofmann, K.P. (1990) Science 250, 123–125.
[29] DeLange, F., Bovee-Geurts, P.H., Pistorius, A.M., Rothschild, K.J. and DeGrip, W.J. (1999) Biochemistry 38, 13200–13209.
[30] Cooper, E.A. and Knutson, K. (1995) in: Physical Methods to Characterize Pharmaceutical Proteins (Herron, J.N., Ed.), pp. 101–142, Plenum Press, New York.
[31] Kisselev, O.G., Kao, J., Ponder, J.W., Fann, Y.C., Gautam, N. and Marshall, G.R. (1998) Proc. Natl. Acad. Sci. USA 95, 4270–4275.
[32] Seitz, H., Heck, M., Hofmann, K.P., Alt, Th., Pellaud, J. and Seelig, A. (1999) Biochemistry 38, 7950–7960.